Polymer 308 (2024) 127359

Contents lists available at ScienceDirect

Polymer

journal homepage: www.elsevier.com/locate/polymer

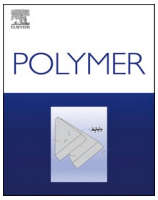

TDAE aromatic oil preference for polymer blends: An analysis of S-SBR, BR, and miscible S-SBR/BR systems

Akansha Rathi [a], Pilar Bernal-Ortega [a], Ahmed G. Attallah [b,c], Reinhard Krause-Rehberg [d], Mohamed Elsayed [b,d], Jürgen Trimbach [e], Cristina Bergmann [e], Anke Blume [a,*]

[a] University of Twente, Faculty of Engineering Technology, Department of Mechanics of Solids, Surfaces & Systems (MS3), Chair of Elastomer Technology & Engineering, Enschede, the Netherlands
[b] Physics Department, Faculty of Science, Minia University, 61519, Minia, Egypt
[c] Helmholtz-Zentrum Dresden-Rossendorf, Institute of Radiation Physics, 01328, Dresden, Germany
[d] Physics Department, Martin Luther University Halle, 06099, Halle, Germany
[e] Hansen&Rosenthal, 20457, Hamburg, Germany

ARTICLE INFO

Keywords:
Treated distillate aromatic extract
Rubber blends
Positron annihilation
Glass transition temperature
Dynamic mechanical analysis
Broadband dielectric spectroscopy

ABSTRACT

This study assesses the impact of Treated Distillate Aromatic Extract (TDAE) oil, at concentrations of 0–20 parts per hundred rubber (phr), on the glass transition temperature (T_g) of High Vinyl/Low Styrene Styrene-Butadiene Rubber (HVLSS-SBR), polybutadiene rubber (BR), and their blends with weight ratios of 70/30 and 50/50. Using Dynamic Mechanical Analysis, Broadband Dielectric Spectroscopy, and Positron Annihilation Lifetime Spectroscopy, we found that TDAE modifies T_g and fractional free volume (F_v) differently across materials. In HVLSS-SBR, TDAE reduced T_g by approximately 10 °C and increased F_v by 0.8 %. In BR, TDAE raised T_g by 5–7 °C without altering F_v. The 70/30 blend showed no T_g change but a 0.6 % F_v increase. For the 50/50 blend, one Havriliak-Negami equation indicated a T_g rise of 2–3 °C and a 0.4 % F_v increase. A two-equation analysis revealed a 6 °C T_g increase and 0.9 % F_v boost in the BR-rich phase, versus a 2 °C rise and 0.3 % F_v uptick in the HVLSS-SBR-rich phase. The sequence of compatibility, influenced by TDAE, is crystalline BR > amorphous BR > HVLSS-SBR >70/30 blend >50/50 blend. This study provides valuable insights into the behavior of TDAE oil in rubber blends and can serve as a basis for further research in this field.

1. Introduction

A tire is an assembly of several components that are built up on a drum and vulcanized in a mold under pressure and heat. It must fulfill the following demands: dimensional stability, durability, driving safety (dry, wet, aquaplaning, winter), comfort (damping, balance, noise), service reliability, economy (abrasion, rolling resistance) and environmental issues. A tire's importance as a safety element necessitates new developments in tire technology in order to keep up with advances in automotive engineering. An additional drive for advancements is the result of legislation for environmental safety and sustainability. Tire design and material improvements are further important contributing factors to the technological advancements in existing tire systems [1]. The three main material-specific requirements relevant to the tread are rolling resistance (RR), abrasion resistance (AR) and wet skid resistance (WSR). The rolling resistance is directly related to fuel economy, the abrasion resistance to service lifetime, and wet skid resistance to driving safety. However, there is a clear trade-off between the three main tire performance indicators: an improvement in one of the three often leads to a deterioration in the other two. A commonly used solution in tread technology is to devise a suitable balance in the tire performance indicators via blending two or three different types of rubber like styrene butadiene rubber, polybutadiene rubber, and Natural Rubber (NR) [1,2].

A tread compound is a complex mixture of rubber, process aids, fillers, and a vulcanization system. Although the microstructure of the rubber has a significant influence on the glass transition temperature (T_g) of rubber, other ingredients also affect the T_g of the compound. This means that the optimization of the trade-off in the performance indicators is not singularly controlled by the rubber's structural and microstructural characteristics, it is rather influenced by further parameters [3].

* Corresponding author.
E-mail address: a.blume@utwente.nl (A. Blume).

https://doi.org/10.1016/j.polymer.2024.127359
Received 7 April 2024; Received in revised form 15 June 2024; Accepted 2 July 2024
Available online 4 July 2024

One factor is the processing aid, which is mostly a mineral-based oil such as Treated Distillate Aromatic Extract (TDAE), in the tire tread formulation. The presence of TDAE, specifically, plays a pivotal role in this optimization by affecting the compound's flexibility and energy dissipation characteristics at different temperatures, which are crucial for maintaining a balance between performance indicators such as rolling resistance, abrasion resistance, and wet skid resistance [4]. Process oils are an indispensable component in the tire compound because they enable the use of higher amounts of filler and higher molecular weight polymers [5]. Besides the improvement in the processability, an improvement in the low temperature properties (decrease of T_g) of a process oil extended compound is regarded as one of the key effects of a process oil for a compound, especially for an application in low temperature conditions like winter tires. However, a decrease of T_g can only be seen when the T_g of the oil is lower than that of the single polymer/blend itself [6]. This is explained based on the Fox's inverse rule of mixtures [7], which states that the oil-extended compound will have a T_g in between that of the oil and the single polymer/blend itself. The TDAE consists of low molecular weight molecules; its presence between the rubber chains has the effect of pushing the chains apart, resulting in a higher free volume (V_f) [8]. Due to the presence of polycyclic aromatic hydrocarbons (PAHs) in mineral-based oils there is an increasing trend towards bio-based process oils [9–11]. To understand the influence of the process oils in detail the challenge is that the commonly used S-SBR/BR based tread compound shows only a single T_g, which makes it difficult to distinguish the degree of influence of the process oil on the individual blend components. This is a major hindrance in determining blend dynamics.

Recent studies have explored the influence of TDAE on rubber-filler interactions in silica-filled SBR/BR blends, revealing that the addition time and content of TDAE can significantly impact the development of the rubber layer and the interfacial interactions [12]. Furthermore, in our previous work, we have delved into the phase dynamics of S-SBR/BR blends, examining how aromatic oils like TDAE partition between the different phases and their effect on the T_g [13,14]. These studies have provided valuable insights into the complex interplay between process oils and rubber blends, informing the design of more efficient and environmentally friendly tire compounds.

In our previous work [14], we primarily focused on understanding how TDAE oil partitions and distributes between the S-SBR and BR phases in blends using broadband dielectric spectroscopy (BDS). We observed that TDAE preferentially plasticizes the BR-rich phase while antiplasticizing the S-SBR-rich phase, as evident from opposite shifts in their respective T_g. The current work significantly expands on those initial findings in several ways:

(i) We have extended the study to pure HVLSS-SBR and pure BR in addition to their blends, allowing us to decouple the effects of TDAE on the individual elastomers.
(ii) We employed multiple complementary techniques - Dynamic Mechanical Analysis (DMA), Broadband Dielectric Spectroscopy (BDS) and Positron Annihilation Lifetime Spectroscopy (PALS) - to comprehensively investigate TDAE's influence on segmental dynamics, T_g shifts, and free volume changes.
(iii) We provide a more in-depth analysis by examining the compatibility between TDAE and the polymers based on adherence to Fox's inverse rule of mixtures for T_g shifts and correlation with the free volume theory of plasticization.
(iv) We have explored blends with different HVLSS-SBR/BR ratios (70/30 and 50/50) to understand how blend composition affects TDAE's preference for the individual phases.

To the best of our knowledge, no directly relevant studies using PALS to investigate the effects of TDAE oil on the segmental dynamics and free volume of HVLSS-SBR, BR, and their blends can be found. However, PALS has emerged as a powerful technique to probe free volume characteristics and interfacial interactions in polymer composites and blends. Previous studies have demonstrated the sensitivity of PALS in detecting free volume hole sizes, concentrations, and their correlation with T_g. For instance, PALS has been used to identify the T_g in a series of poly(n-alkyl methacrylate)s [15]. Moreover, the microstructure of the free volume and its temperature dependence in fluoroelastomeric copolymers of tetrafluoroethylene (TFE) and perfluoro(methyl vinyl ether) (PMVE), PFE, as well as vinylidene fluoride (VDF) and hexafluoropropylene (HFP) (VDF78/HFP22), have been demonstrated by PALS [16]. PALS-derived T_g values agree well with those obtained from techniques like PVT, DSC, and DMA for many amorphous and semi-crystalline polymers, such as polystyrene [17]. Therefore, the utilization of PALS in the current work will complement the results of the other techniques and help understand the role of the oil in the behavior of the studied polymers and their blends.

Table 1
Formulation and mixing procedure of the studied compounds.

Ingredient			Amount (in phr)
Low styrene S-SBR			100/70/50/0
High *cis*-BR			0/30/50/100
Zinc Oxide (ZnO)			4
Stearic Acid (SA)			3
N-cyclohexyl-2-benzothiazole sulfenamide (CBS)			2.5
Sulfur (S)			1.6
TDAE			0/10/20
1st Stage: Internal Mixer Brabender Plasticorder 350S 50 RPM; 50 °C; Fill factor: 0.7			2nd Stage: Two-roll mill Polymix 80T Friction ratio: 1.25:1; ca. 40 °C
0 phr TDAE (Min. s.) 0.30 Add polymers 1.30 Add ZnO and stearic acid 4.00 Dump	**10 phr TDAE** (Min. s.) 0.30 Add polymers 1.30 Add ZnO and stearic acid 2.30 Add 3/4th TDAE 4.30 Add 1/4th TDAE 6.30 Dump	**20 phr TDAE** (Min. s.) 0.30 Add polymers 1.30 Add ZnO and stearic acid 2.30 Add 3/8th TDAE 4.30 Add 3/8th TDAE 7.30 Add 1/4th TDAE 9.30 Dump	**All samples** (Min. s.) 0.30 Add curatives 5.00 Dump

2. Experimental section

2.1. Materials

The materials used in this study are low styrene S-SBR: SPRINTAN™ SLR 4602 (Synthos, Schkopau, Germany); high *cis*-BR: BUNA CB24 (Lanxess Deutschland GmbH, Leverkusen, Germany); Treated Distillate Aromatic Extract (TDAE): VIVATEC 500 (Hansen & Rosenthal KG, Hamburg, Germany). Some important analytical properties of the S-SBR, BR and TDAE are presented in Table 1.

The curing system employed consists of zinc oxide, stearic acid and sulfur from Sigma Aldrich (St Louis, USA); N-cyclohexyl-2-benzothiazole sulfenamide (CBS) from Flexsys (Brussels, Belgium). All chemical reagents were used as received.

2.2. Compounding, mixing, and curing

The rubber compounds analyzed in this study were prepared in a two-step mixing procedure. The first stage was performed in an internal mixer Brabender Plasticorder 350 (Duisburg, Germany) with a fill factor of 0.7, rotor speed of 50 rpm and initial temperature of 50 °C. The second stage was done in a two-roll mill Schwabenthan Polymix 80T (Berlin, Germany) with a friction ratio of 1.25:1 and a temperature of 40 °C.The samples were prepared according to the formulation presented in Table 1. The addition of filler was excluded from this study to avoid any interference.

The samples were vulcanized in a hydraulic press (*Wickert WLP 1600*) at 100 bar and 160 °C to form sheets with a thickness of 2 mm, according to their t_{90} + 2 min optimum vulcanization times, as determined with a Rubber Process Analyzer (*RPA 2000, Alpha Technologies*), following ISO 3147:2008 at 160 °C. Additionally, 0.1–0.2 mm thick sheets were also vulcanized according to their respective t_{90} values at 160 °C for BDS measurements.

The compounds are referred to in a simplified form (Table 2) as follows:

2.3. Methods

Dynamic Mechanical Analysis (DMA). Dynamic Mechanical Analysis (DMA) of the vulcanized samples was carried out in tension mode in a Metravib DMA2000 dynamic spectrometer. The measurements were performed from −120 °C to +80 °C in steps of five degrees at a dynamic strain of 0.5 % and frequency of 1 Hz on samples of (25·5·2) mm. The accuracy of the temperature controller is ±0.1 °C, the phase angle is ±0.1° and the frequency is ±0.01 %. The accuracy of the determination of T_g was ±1 °C in each case.

Broadband Dielectric Spectroscopy (BDS). BDS measurements were performed on a Broadband Dielectric Spectrometer with the ALPHA-A High Performance Frequency Analyzer of Novocontrol Technologies. The vulcanized 0.1–0.2 mm sheets were cut into disk shapes and were mounted in the dielectric cell between two parallel gold-plated electrodes. For the TDAE, a special cell designed for studying dielectric properties of liquids was used. The complex dielectric permittivity, ε^* ($=\varepsilon' - i\varepsilon''$), being composed of, ε' the real part and ε'' the imaginary part, was measured by performing consecutive isothermal frequency sweeps, 10^{-1}-10^{6} Hz in the temperature range from −120 °C to +80 °C in steps of 5 °C. The temperature was controlled to better than 0.1 °C using a Novocontrol Quatro cryosystem; the error of the ALPHA impedance measurement was less than 1 %.

Positron Annihilation Lifetime Spectroscopy. The positron annihilation lifetime spectroscopy (PALS) [18–20] measurements were performed using a digital lifetime spectrometer with a time resolution of 170 ps [21,22], where a 740 kBq ^{22}Na positron source protected by 7.5 μm thick Kapton foil was sandwiched between two identical samples each 2 mm thick. This arrangement was wrapped in Al-foil and placed in the sample holder. The samples were measured in the temperature range of −140 to +60 °C. 5×10^6 counts were accumulated in each positron lifetime spectrum. The error in the measurement is less than 0.4 %. The raw positron lifetime spectra were analyzed by the lifetime LT 9 program [23]. For more details about PALS outputs and calculating hole volume and free volume fraction, see section S.2.

Table 2
Designated naming system of the studied compounds.

Compound	Referred as in text:
Single polymers: S-SBR and BR with 0/10/20 phr of TDAE	
S-SBR	S-SBR_0; S-SBR_10; S-SBR_20
BR: Amorphous-rich BR (BR-A)	BR-A_0; BR-A_10; BR-A_20
BR: Crystallite-rich BR (BR-C)	BR-C_0; BR-C_10; BR-C_20
S-SBR/BR 70/30 and 50/50 blends with 0/10/20 phr TDAE	
70/30	70/30_0; 70/30_10; 70/30_20
50/50	50/50_0; 50/50_10; 50/50_20
50/50 (BR-rich)	BR-rich_0; BR-rich_10; BR-rich_20
50/50 (Blend-rich)	Blend-rich_0; Blend-rich_10; Blend-rich_20

3. Results

The results section is structured by technique, starting with the results of each individual polymer and moving on to the results of the polymer blends for each of the three techniques used: DMA, BDS, and PALS. This enables a thorough comparison of the outcomes for both the individual polymers and their blends while providing a clear and succinct review of the important findings from each technique.

3.1. DMA measurements

TDAE on the S-SBR and the BR compounds. As mentioned before, based on the theoretical predictions from the Fox equation an improvement in low temperature properties (decrease in T_g) in the final compound can only be observed for rubbers with a higher T_g value compared to that one of the process oil used. Since the T_g of BR is lower and the T_g of S-SBR is higher than the T_g of TDAE, it is expected that an improvement in the low temperature properties can only be seen for the TDAE extended S-SBR compounds. It is clear from the DMA measurements that a decrease in the T_g of S-SBR compounds and an increase in the T_g of the BR compounds has indeed been observed by adding TDAE oil: see Fig. 1 [24,25]. In addition to the T_g peak of BR, a distinct crystallization peak can be seen between −60 and −40 °C in the DMA curve due to the ability of the long chain molecules to crystallize. In non-branched polymers such as high-cis BR the polymer chains can rearrange to form spherical semi-crystalline regions which are called spherulites [26]. The formation of the spherulites in the high *cis*-BR can be identified as the crystallization peak: see Fig. 1-C.

An increase in the height of the peak corresponding to the crystallization process can be seen with addition of 10 phr TDAE oil, which decreases again with the further addition of another 10 phr. It is assumed that the addition of 10 phr TDAE results in an increase in the free volume, creating more space for the BR chains to move freely and rearrange to form spherulites. It is possible that the addition of an additional 10 phr oil can create a hindrance to the process of rearrangement of the BR chains to form spherulites. Thus, a decrease in the height of the peak corresponding to crystallization is seen from the DMA measurements.

The observed effect of TDAE on T_g [25] of the pure SBR and pure BR compounds is in accordance with the Fox's inverse rule of mixtures [6], which suggests that the shift in the T_g of the oil-extended polymer is towards the T_g of the additive (TDAE). Since the T_g of the TDAE (−49 °C) is lower than the T_g of S-SBR and higher than the T_g of the BR, it expected to decrease the T_g of the oil-extended S-SBR and increase the T_g of the oil-extended BR. The driven T_g values from Fig. 1 are presented in Table 3.

The main conclusion from the DMA measurements is that the

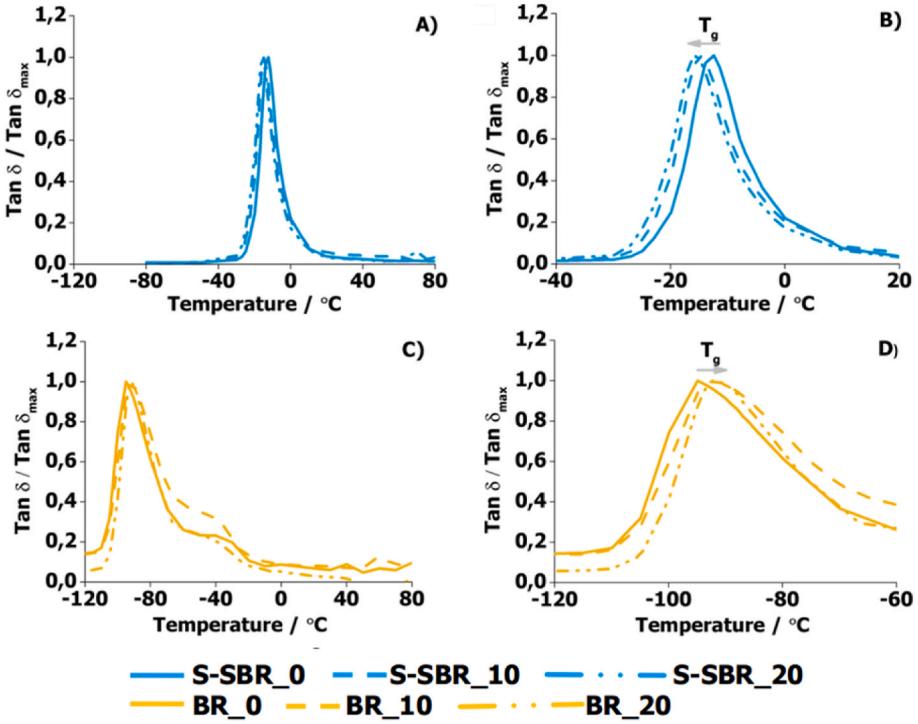

Fig. 1. Normalized tan δ vs. temperature curves for the effect of the addition of 0/10/20 phr TDAE on A) S-SBR (−120 to 80 °C), B) S-SBR (in the range of T_g), C) BR (−120 to 80 °C), and D) BR (in the range of T_g).

Table 3
T_g from DMA for the oil extended pure S-SBR and pure BR compounds.

Amt. of TDAE/phr	Tg (S-SBR)/°C	Tg (BR)/°C
0	−12	−95
10	−15	−93
20	−16	−92

addition of TDAE leads to a plasticization effect on S-SBR and an anti-plasticization effect on BR. In the oil-extended S-SBR, it is possible that the addition of the TDAE oil has the effect of pushing the chains apart to increase the net free volume, which makes the segmental motion easier. In the oil-extended BR, it is possible that the addition of TDAE, which contains ca. 25 wt% bulky aromatic compounds, leads to a restriction in the segmental motion of the otherwise highly linear and mobile BR chains. These observations will be compared in the following part with the measurement results of T_g from BDS and PALS. Additionally, the effect of TDAE on the free volume will be evaluated by PALS measurements, which can estimate the fractional free volume at the T_g of the oil-extended compounds.

TDAE on the S-SBR/BR blends. The effects of TDAE on two different S-SBR/BR blends are investigated. For the 70/30 blend, the DMA measurement data is presented in Fig. 2A, top (the entire range of temperatures from −120 to 80 °C) and Fig. 2B, top (zoomed in the range of T_g). According to the Fox's inverse rule of perfect mixtures, a minor shift to lower temperatures is seen with the addition of TDAE oil. T_g values for the 70/30 blend from DMA are −34 °C and −49 °C, respectively. As a result, a plasticizing effect of the TDAE oil on the 70/30 blend is detected. For the 50/50 blend in Fig. 2A, bottom (the entire range of temperatures from −120 to 80 °C) and Fig. 2B, bottom (zoomed in the range of T_g), the addition of TDAE oil leads to a slight shift to higher temperatures, as seen from the DMA measurement data. Given the difference between the T_g of the 50/50 blend made from DMA (−54 °C) and the T_g of the TDAE oil (−49 °C), this change is also predicted based on the Fox's inverse rule of perfect mixtures indicating that the TDAE oil has an anti-plasticization impact on the 50/50 blend. In BR/SBR blends, crystallization is reduced for low SBR amounts and seems to disappear totally for 50/50 blends. This behavior was already found in literature [27].

3.2. BDS measurements

TDAE on the S-SBR and the BR compounds. All the experimentally obtained dielectric loss (ε'') vs frequency spectra for S-SBR and BR compounds are fitted using the Havriliak-Negami (HN) equation [28]:

$$\varepsilon^*_{HN}(\omega) = \varepsilon_\infty + \frac{\Delta\varepsilon}{\left(1 + (i\omega\tau_{HN})^b\right)^c} \quad (1)$$

where τ_{HN} is the characteristic HN relaxation time, which represents the most probable relaxation time from the relaxation time distribution function, ω is the angular frequency, Δε is the relaxation strength ($\Delta\varepsilon = \varepsilon_S - \varepsilon_\infty$) where ε_S and ε_∞ are related to the complex dielectric function at low and high frequencies respectively, $\varepsilon^*_{HN}(\omega)$ is the frequency dependent Havriliak-Negami complex dielectric permittivity, and b and c are shape parameters, which describe the symmetric and asymmetric broadening of the relaxation time distribution function, respectively. The HN fittings are done at various temperatures where the peak of segmental relaxation is clearly observable. The fitting is done using the WINFIT software from Novocontrol technologies. The adjustable parameters obtained from the HN fitting are: the relaxation strength (Δε), which is related to the number density of the polarizable species between the electrodes; the characteristic HN relaxation time (τ_{HN}), which represents the most probable relaxation time from the relaxation time distribution function (Tables S1 and S2). The corresponding T_g for each system is calculated by extrapolation of the data points corresponding to the segmental dynamics using the fittings based on the Vogel-Fulcher-Tamman (VFT) equation [29]:

$$\tau_{max} = \tau_0 \, exp\left(\frac{B}{T - T_0}\right) \quad (2)$$

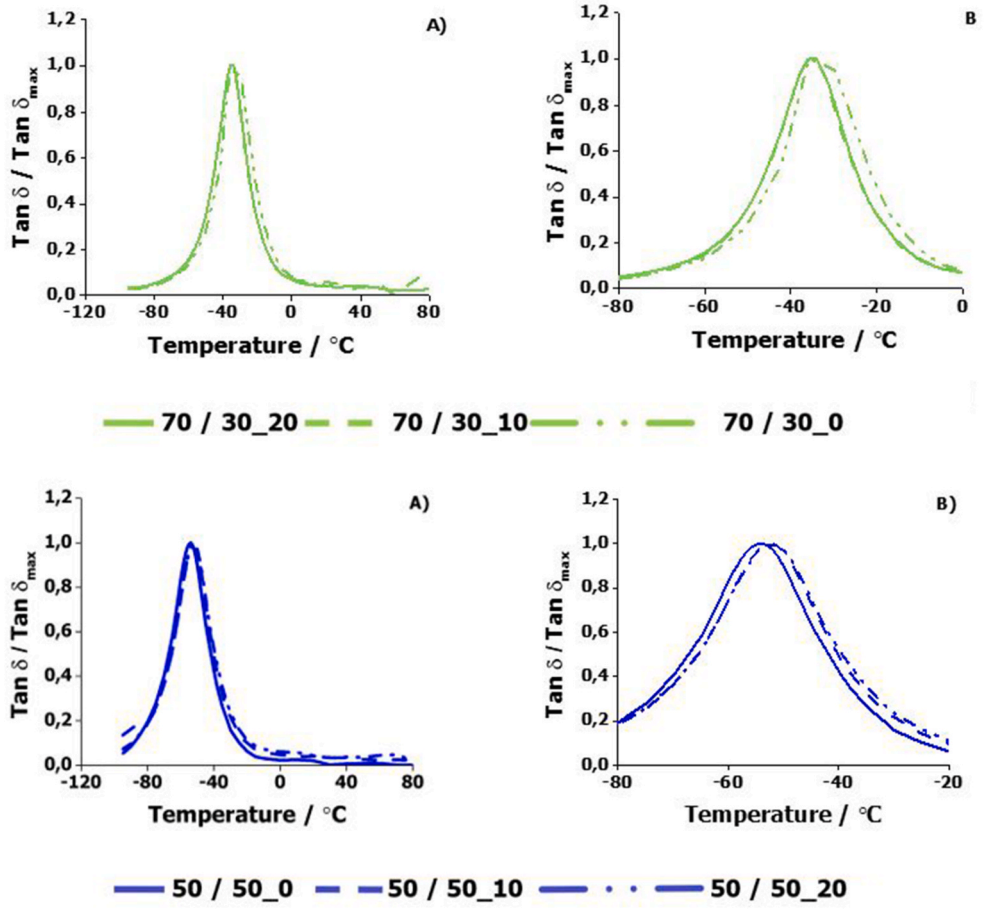

Fig. 2. Normalized tan δ vs. temperature curves for the effect of the addition of 0/10/20 phr TDAE
Top panel: S-SBR/BR 70/30 blend: A) in the entire range of −120 to 80 °C), B) zoomed in the range of T_g.
Bottom panel: the S-SBR/BR 50/50 blend A) in the entire range of −120 to 80 °C), B) zoomed in the range of T_g.

where, $\tau 0$ and B are empirical parameters, and T_0 is the ideal glass transition or Vogel temperature, which is generally 30–70 K below T_g. A universal value of $\log \tau_0 = -14$ was adapted for the data fitting using the VFT equation [30]. The VFT equation has been developed with the consideration of the free volume model of the glass transition [31–34]. Therefore, the main features of the VFT equation can be explained using the free volume model. A polymer molecule occupying a certain volume "v" is restricted in its motion within this volume by its nearest neighbors. When the "v" reaches a critical value "v_c", the excess volume is considered as the free volume "v_f". The movement of a polymer chain between two sites can only happen when a free volume greater than a minimum free volume "v_f" is available. The temperature corresponding to the value "-2" on the y-axis of Fig. 2 is taken as the T_g from BDS [35]. The choice of the temperature is based on the correspondence of the value at "-2" (which means a frequency of 10^{-2} Hz) with the frequency associated with the measurement from Differential Scanning Calorimetry (DSC).). The whole further evaluation was done according to Ref. [36]. One limitation of the whole evaluation is that it is not possible to determine the average relaxation times over the full temperature ranges.

There are two types of relaxations present in the unfilled S-SBR and the BR compounds: the segmental level relaxation or the glass transition

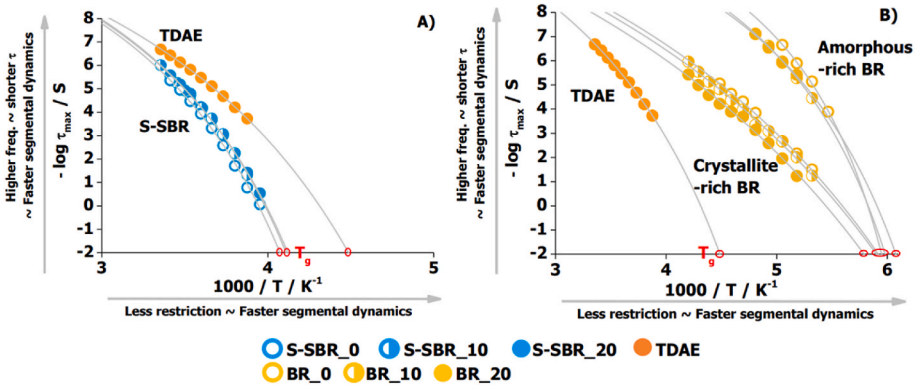

Fig. 3. Temperature dependence of the average relaxation times of pure TDAE, A) S-SBR and B) BR compounds with 0/10/20 phr of TDAE oil.

(T_g) process, and the monomer level relaxation or the β-relaxation. Although both relaxations are present in the oil-extended compounds, the focus here is on the effect of the oil on the segmental dynamics (T_g) [37,38]. The β-relaxation is not elaborated on here as these monomer-scale relaxations are not affected by the addition of oil. An activation plot showing the temperature dependence of the relaxation times of the TDAE oil, the non-oil-extended, and TDAE oil-extended S-SBR and BR compounds was plotted in Fig. 3.

From the activation plot, the effect of the TDAE oil on the segmental dynamics of the S-SBR and the BR compounds can be seen. In general, if the peak of the segmental dynamics moves towards higher frequencies of a BDS frequency sweep, it indicates that the relaxation time of the segments gets shorter. Therefore, a movement of the data points at a fixed temperature towards shorter relaxation times implies faster segmental dynamics (improvement in low temperature properties). Similarly, at a fixed relaxation time, the data points corresponding to the segmental dynamics of a compound move to lower temperatures, which means a lower restriction and hence faster segmental dynamics.

The data points of the segmental dynamics of the S-SBR move to slightly shorter relaxation times (at a fixed temperature) and lower temperatures (at fixed relaxation time) inside the activation plot with the addition of TDAE. This indicates a decrease in T_g (see also Table 4) and an improvement in low temperature properties. This effect can be considered as a plasticization effect. The effect of the TDAE on the BR compounds can be seen in the form of an individual effect on the amorphous-rich and the crystallite-rich phases of the BR. This interpretation will be further supported by the PALS data, presented in chapter 3.3. By adding TDAE, the data points corresponding to the segmental dynamics of the amorphous-rich phase do not follow a clear trend. However, upon extrapolation using the VFT fittings, a decrease in T_g of the TDAE-extended amorphous-rich BR compared to the non-oil-extended amorphous-rich BR can be seen (see Table 3). This indicates a plasticization effect on the amorphous-rich BR phase. While with adding TDAE, the segmental dynamics of the crystallite-rich phase move to longer relaxation times (at a fixed temperature) and higher temperatures (at fixed relaxation time), an increase in T_g is observed which indicates a deterioration in low temperature properties: an anti-plasticization effect.

The main conclusion from the BDS measurements is that the addition of TDAE leads to a plasticization effect on the S-SBR and the amorphous-rich phase of BR and an antiplasticization effect on the crystallite-rich phase of BR. As mentioned in the previous part with the DMA measurements, the effect of TDAE pushing the polymer chains apart by the addition of TDAE can explain the plasticization effect on the S-SBR and the amorphous-rich phase of BR. It is also possible that the TDAE oil (containing ca. 25 wt% bulky aromatic components) can further restrict the segmental dynamics of the BR chains interacting with the spherulites of BR. This might explain the anti-plasticization of the crystallite-rich phase of BR by the addition of the TDAE oil. A further clarification will be achieved by measuring the effect of the TDAE on the free volume at T_g of the S-SBR and the BR phase by PALS measurements.

TDAE on the S-SBR/BR blends. The analysis of the measurement data from BDS was done in the same way as explained in the previous part. The dielectric loss (ε") peaks at various temperatures in the range of the segmental dynamics of the non-oil-extended and the oil-extended blend could be fitted with a single HN equation as the blend expressed itself as a single peak on the BDS frequency and temperature sweeps. The different parameters obtained from the single HN fittings for the non-oil-extended and the oil-extended 70/30 as well as the non-oil-extended and the oil-extended 50/50 blends are presented in Table S4. The results of the HN fit can also be translated to the activation plot: see Fig. 4. A and B. On the activation plot the data points corresponding to the non-oil-extended and the oil-extended 70/30 blends are seen to overlap (Fig. 4A). On extrapolation using (VFT fitting) for obtaining the value of T_g also it is evident that the segmental dynamics of the non-oil-extended and the oil-extended 70/30 blends is the same [24,25].

The dielectric loss (ε") peaks at various temperatures in the range of the segmental dynamics of the 50/50 blend could be fitted with a single HN equation as the blend expressed itself as a single peak on the BDS frequency and temperature sweeps and two HN equations (to de-convolute the single peak representing the combined dynamics of the S-SBR and the self-concentrated BR units). The further discussion of the effect of the addition of 0, 10 and 20 phr of the TDAE oil is divided in two parts:

i) *Effect of the TDAE when one HN eqn. is used to fit the frequency sweep data for the S-SBR/BR 50/50 blend:* The BDS data from this part will be compared to the DMA data.
ii) *Effect of the TDAE when two HN eqns. are used to fit the frequency sweep data for the S-SBR/BR 50/50 blend (De-convolution approach):* The de-convolution approach for fitting two contributions within the broad peak of the dielectric loss ε" (at various temperatures in the temperature range of the segmental relaxation) in the frequency sweep. From this fitting protocol, two contributions are identified: one is the blend-rich phase with a behavior similar to the one HN equation fitted 50/50 blend and the other is the BR-rich phase with a behavior similar to the crystallite-rich phase of the pure BR. The BDS data from this part will be compared to the PALS data.

i) *Effect of the TDAE when one HN eqn. is used to fit the 50/50 blend*

The different parameters obtained from the single HN fitting are presented in Table 4. The results of the HN fit are translated to the activation plot: see Fig. 4B. On the activation plot the data points corresponding to the non-oil-extended and the oil-extended 50/50 blends are almost overlapping. On addition of 10 phr TDAE oil, the data points corresponding to the segmental dynamics of the 50/50 blend extended with 10 phr of TDAE oil are almost overlapping with the non-oil-extended compound: see Fig. 4B and Table 5. On addition of 20 phr TDAE oil, the data points corresponding to the segmental dynamics of the 50/50 blend extended with 20 phr of TDAE oil are shifted towards a higher temperature (at a fixed relaxation time) on the x-axis and slightly higher relaxation time (at a fixed temperature) on the y-axis: see Fig. 4B and Table 5. This means that the segmental dynamic of this compound is more restricted than that of the non-oil-extended compound.

ii) Effect of the TDAE when two HN eqns. are used to fit the 50/50 blend (De-convolution approach)

To explore the effect of the TDAE oil on the separate components (the blend-rich and the BR-rich) of the 50/50 blend the broad dielectric loss peak in the BDS frequency sweep can be de-convoluted into the blend-rich phase (α′) and the self-concentrated BR-rich phase (α). The HN parameters: Δεα, Δεα', b, b′, c, c′, τ_{HN} (α) and τ_{HN} (α′) for each contribution are shown in Table S5. The HN parameters are then translated to the activation plot which shows the temperature dependence of the relaxation time for the α and α′ relaxation processes: see Fig. 5. On the activation plots it is noticed that especially at lower temperatures there is an increase in the relaxation time for both oil-extended blend phases: the blend-rich and the BR-rich. This means that the addition of the TDAE oil leads to slow down the segmental dynamics of both phases, the blend-rich and BR-rich ones. On extrapolation of the data points corresponding to the segmental dynamics of the non-oil-extended and the oil-

Table 4
T_g from BDS obtained from the extrapolation of the data points corresponding to the segmental dynamics with the Vogel-Fulcher-Tamman (VFT) fittings.

Amt. of TDAE /phr	Tg (S-SBR) /°C	Tg (BR-A)/°C	Tg (BR-C) /°C	Tg (TDAE) /°C
0	−28	−105	−104	−50
10	−30	−106	−104	
20	−31	−109	−100	

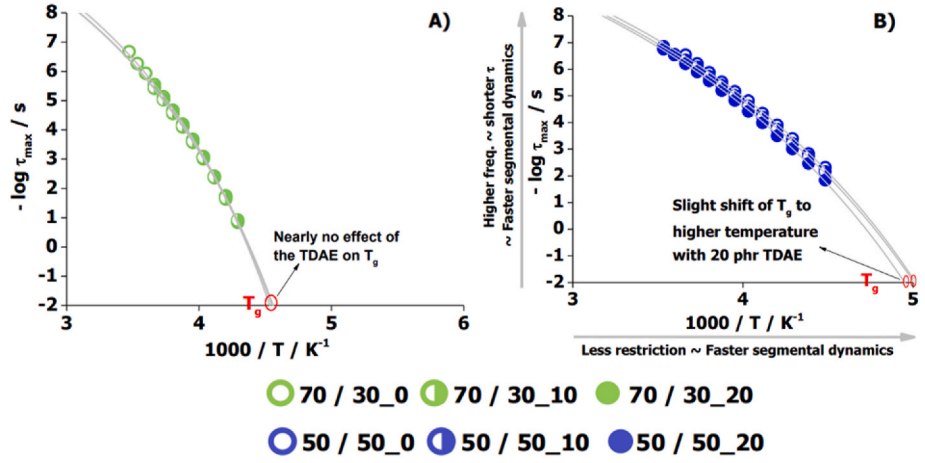

Fig. 4. Temperature dependence of the average relaxation times of A) S-SBR/BR 70/30 and B) S-SBR/BR 50/50 wt ratio blends with 0/10/20 phr of TDAE oil.

Table 5
T_g values for the 50/50 blend with 0/10/20 phr TDAE oil from DMA and BDS measurements.

Compound	Tg^{DMA}/°C	Tg^{BDS}/°C
50/50_0	−54	−74
50/50_10	−53	−73
50/50_20	−52	−71

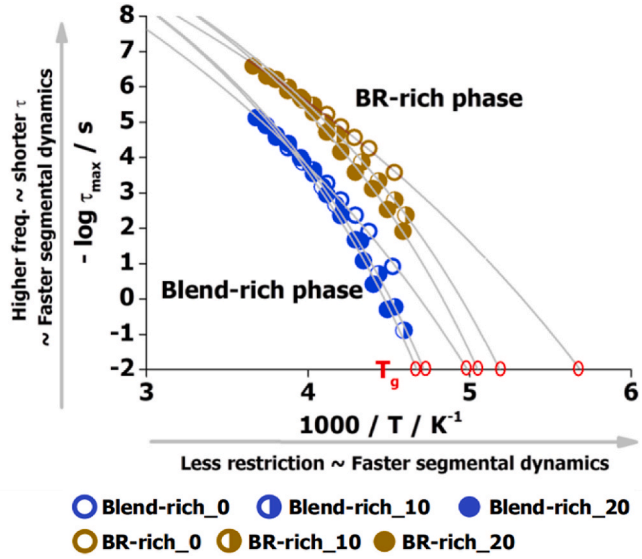

Fig. 5. Temperature dependence of the average relaxation times of S-SBR/BR 50/50 wt ratio blends with 0/10/20 phr of TDAE oil.

extended blend phases using the VFT fittings, it is possible to obtain the value of T_g: see the T_g values presented in Table 4.

3.3. PALS measurements

TDAE on the S-SBR and the BR compounds. In amorphous polymers there is an accompanied change in the free volume size and intensity as the phase changes from glassy to rubbery. This point of change in the slope in the F_v *vs* temperature curves is taken as the glass transition temperature (T_g) [39]. We presented the corresponding PALS parameters of the non-oil-extended S-SBR and the TDAE on S-SBR in Tables S3 and S4 as examples. The PALS measurement has also been carried out for the pure TDAE oil to estimate its T_g and the F_v associated with the T_g: see

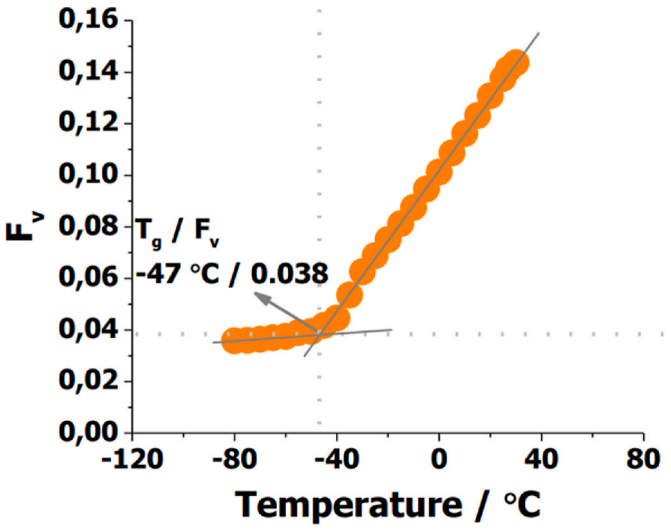

Fig. 6. Fractional free volume F_v as a function of temperature for TDAE oil.

Fig. 6. For the pure TDAE oil, there is one change of slope at the lower temperature (−47 °C) corresponding to the T_g. For the non-oil-extended S-SBR compound there is one change in the slope at the lower temperature side corresponding to the T_g: see Fig. 7A. For the non-oil-extended BR compound there are two identifiable phases similar to the results from DMA and BDS measurements: the amorphous-rich (~−100 °C) and the crystallite-rich (~−50 °C) phase: see Fig. 7D. Additionally, there is a change of slope at ca. −100 °C which follows a steep increase in the F_v: see Fig. 7D. This is considered to be the amorphous-rich BR phase undergoing the glass to rubber transition. With the increase in F_v up to 0.028 at a ca. −50 °C, there is enough room for the BR chains to re-arrange into a spherulitic morphology: see Fig. 7D. This is the point where a part of the BR chains crystallizes to form a spherulitic morphology. The remaining part of the BR becomes more mobile accompanied by a still increasing F_v. There is an additional change of slope at ca. −10 °C. It is taken as the saturation temperature (T_S) which is due to the quasi-saturation of τ_3. It happens either due to the fact that the matrix is too soft and hence the o-Ps cannot find rigid walls around it or it is due to the fact that τ_3 becomes comparable to the relaxation time of molecular chains and cannot be clearly distinguished [40–42]. Ideally, in the range between T_g and T_S the temperature-dependent o-Ps lifetime increases linearly with the increase of the temperature, indicating a direct correlation between the free volume size and the given temperature in fully amorphous systems [40].

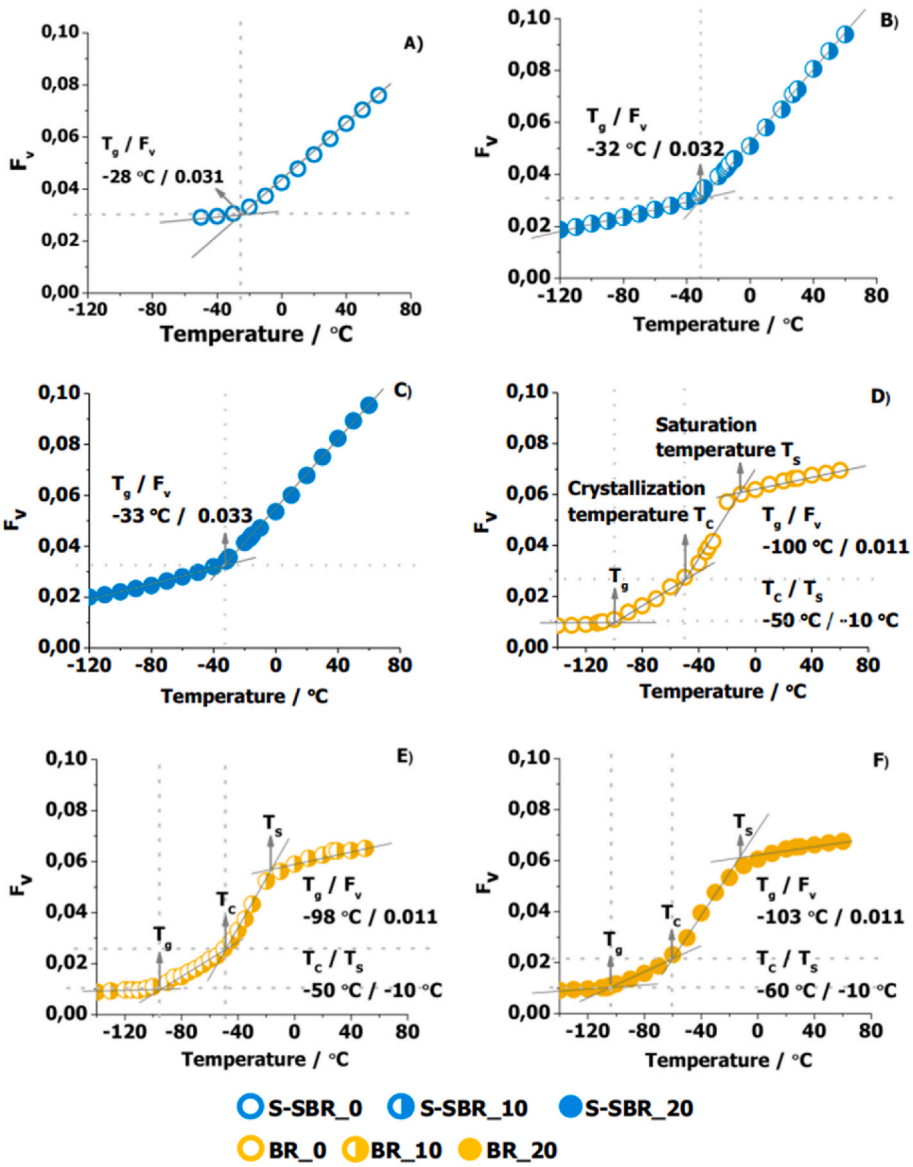

Fig. 7. Fractional free volume F_v as a function of temperature for S-SBR with different amounts of TDAE A) 0 phr, B) 10 phr, C) 20 phr; and BR with different amounts of TDAE D) 0 phr, E) 10 phr, F) 20 phr.

With the addition of an increasing amount of TDAE, a decrease in the T_g of the oil-extended S-SBR is observed. This is the same effect as seen from the DMA and BDS measurements. Furthermore, in the PALS measurement data there is a slight increase in the fractional free volume (F_v) accompanying the shift in the T_g of the TDAE-extended S-SBR compounds: see Fig. 7A–C. The magnitude of the increase in the F_v for the oil-extended S-SBR compounds is in the order of 0.002. Since the measurement error is ±0.00023 (less than 0.4 %), this difference seems to be meaningful. Then, the increase in F_v at T_g can be explained by the presence of TDAE having the effect of pushing polymer chains apart, thus leading to an increase in F_v along with a decrease in T_g. This is in accordance with the free volume theory of plasticization [39]. Therefore, it can be concluded that an overall plasticization effect exists of the TDAE oil on the S-SBR chains.

In the case of TDAE-extended BR compounds the discussion can be divided into the effect of the TDAE on the amorphous-rich and the crystallite-rich phase. With the addition of 10 phr of TDAE oil, there is a slight increase in the T_g (without a change in F_v) of the amorphous-rich phase and no effect on the crystallization temperature (T_C) of crystallite-rich phase: see Fig. 7. D and E. With further addition of a total of 20 phr of the TDAE, there is a slight decrease in the T_g (without a change in the F_v) of amorphous-rich phase and a decrease in the crystallization temperature (T_C) of crystallite-rich phase: see Fig. 7D and F. The shift in the T_g of the amorphous-rich BR phase on the addition of the TDAE oil is insignificant in terms of the absolute values. Since the glass to rubber transition is a process that happens over a range of temperatures, the observed change in the T_g in the oil-extended BR compounds can be considered within the limits of the glass transition (T_g) process. Therefore, it can be concluded from the PALS measurements that there is no effect from the addition of the TDAE oil on the amorphous-rich phase of BR.

A more significant difference is observed between the crystallization temperature (T_C) and the accompanying fractional free volume. With the addition of 10 phr of TDAE, there is no effect on the absolute value of T_C (~−50 °C). However, a decrease in the accompanying fractional free volume to the T_C is observed: see Fig. 7D and E. With the further addition of a total of 20 phr of TDAE oil, the T_C (~−60 °C) shifts to much lower temperatures and a further decrease in the accompanying fractional free volume is observed: see Fig. 7D–F. It seems that the incorporation of the TDAE oil slows down the increase in the fractional free volume between

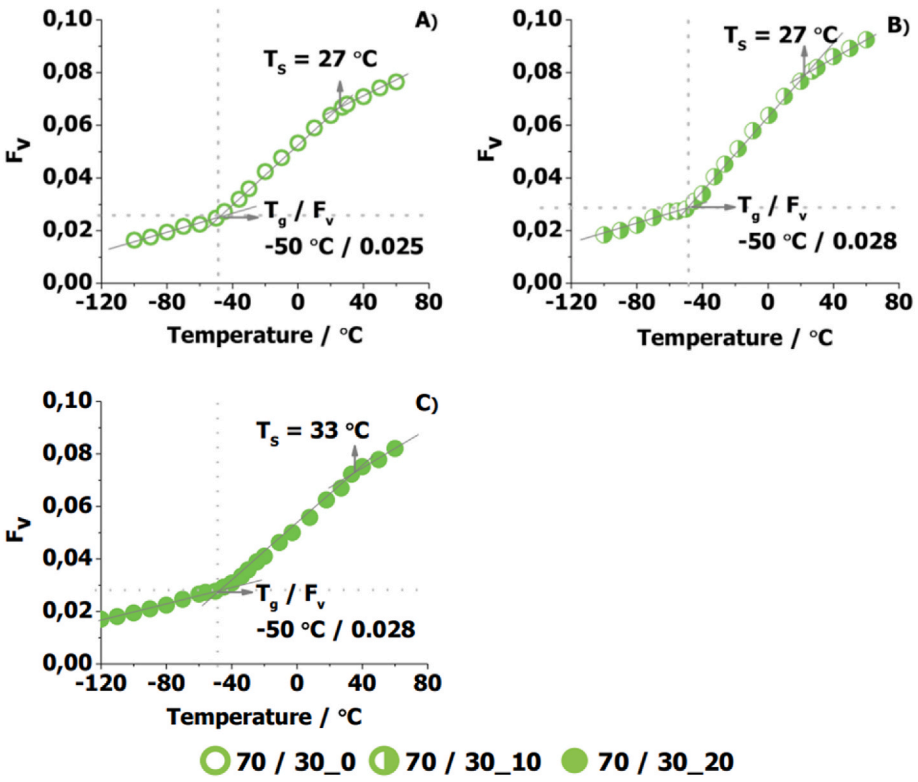

Fig. 8. Fractional free volume F_v as a function of temperature for S-SBR/BR 70/30 wt ratio blends with different amounts of TDAE.

the T_g and the T_C by occupying the free volume sites: see Fig. 7D–F. This could result in a net reduction in the fractional free volume of the oil-extended BR compounds.

TDAE on the S-SBR/BR blends. From the PALS measurements, little or no shift in the T_g of the 70/30 blend is seen with the addition of 0, 10 and 20 phr of TDAE oil: see Fig. 8. However, an increase in the fractional free volume F_v at T_g with the addition of 10 and 20 phr TDAE to the 70/30 blend is noticed. This means that although the value of the T_g does not change with the addition of TDAE, there is still an increase in F_v to accommodate the oil molecules. It is possible that the high miscibility of the S-SBR and BR chains makes it difficult to modify the segmental dynamics of the blend with only 20 phr of TDAE oil.

The obtained T_g and F_V from PALS for the individual blend-rich and BR-rich phase of the 50/50 blend are depicted in Fig. S5. The T_g corresponding to the blend-rich phase and BR-rich phase can be identified on these curves. The respective T_g of the blend (Blend-rich) and the self-concentrated BR (BR-rich) in the blend are subsequently calculated: see Table 6. This supports the results from the de-convolution approach of BDS as well provides an insight into the respective changes in the fractional free volume (F_v) associated with the T_g of each phase: see Fig. S2. The T_g of both the blend-rich and the BR-rich phase increases with the addition of 10 and 20 phr of TDAE. A detailed consideration of the changes in F_v at T_g shows that the F_v increases steadily for both the BR-rich and the blend-rich phases with the addition of the TDAE oil: see Table 6. The increase in the F_v is at the level of the third decimal point which is still a significant change in these measurements due to a measurement error of ±0.00023 (less than 0.4 % error). The surprising point is that normally when the free volume increases, the T_g correspondingly decreases due to the higher amount of available space for the movement of polymer chains. In this case, the T_g increases and the corresponding F_v increases, which is contradictory behavior. It is possible that the variety of molecules (paraffinic, naphthenic, aromatic) present in the TDAE oil, especially aromatic molecules being bulky molecules can effectively increase the distance between the polymer chains due to steric hindrance. This effectively increases the free volume in a compound. A possible explanation for the shift in the T_g of the oil-extended compound is that the inclusion of these bulky molecules in the blends restricts the segmental mobility thereby increasing the T_g. Another possibility is that based on Fox's inverse rule of mixtures an increase in the T_g of both phases is expected as the T_g of the both phases (−96 and −72 °C) in the non-oil-extended blend is lower than the T_g of the TDAE oil itself (−49 °C).

Table 6
T_g/F_v of the Blend-rich and BR-rich processes of the 50/50 blend, experimentally obtained from BDS and PALS measurements, with uncertainty of Tg-PALS of ±1.2 °C.

Compound		T_g^{BDS}/°C	T_g^{PALS}/°C	Fv
50/50_0	BR-rich	−97	−96	0.015
	Blend-rich	−72	−73	0.021
50/50_10	BR-rich	−80	−82	0.018
	Blend-rich	−61	−60	0.025
50/50_20	BR-rich	−75	−80	0.021
	Blend-rich	−59	−60	0.027

4. Discussions

In this research, the influence of the TDAE oil on the segmental dynamics and the T_g of (a) the oil-extended S-SBR and (b) BR compounds and their blends with two different mass ratios (c) 70/30 and (d) 50/50 have been studied with three different techniques: DMA, BDS and PALS.

(a) In the oil-extended S-SBR compounds, a slight decrease in the T_g is observed by all three methods with the addition of every 10 phr of the TDAE oil (Fig. 9A). This is an expected result based on the Fox's inverse rule of perfect mixtures considering the difference in the T_g of the S-SBR and the T_g of the TDAE oil. From the PALS measurement, an accompanying increase in the fractional free volume at the T_g can also be seen. Therefore, it is concluded that there is a plasticization effect of the TDAE on the S-SBR chains.

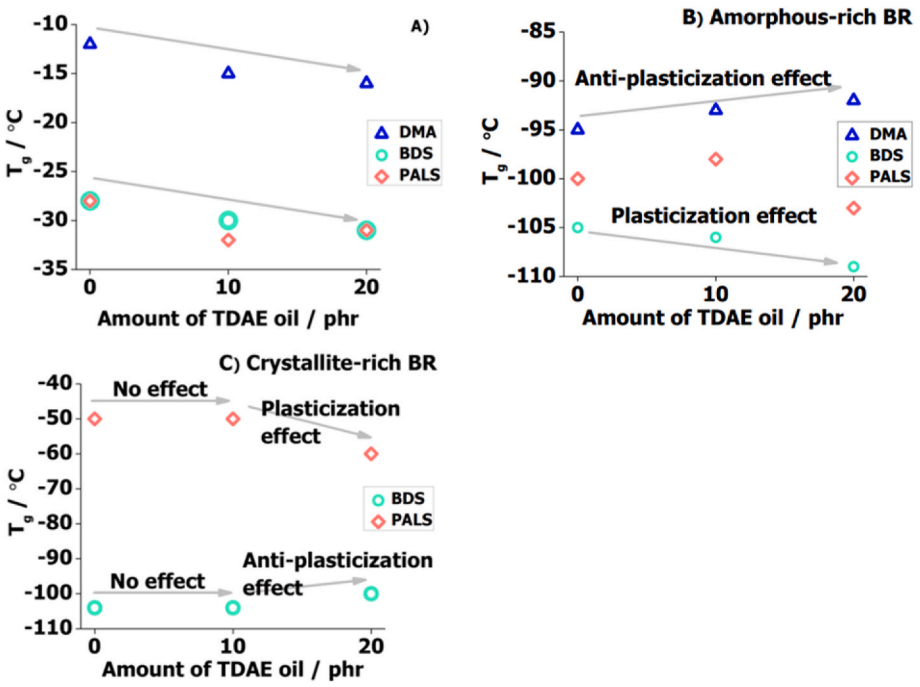

Fig. 9. Comparison of the shift in T_g from DMA, BDS and PALS on the addition of the 0/10/20 phr of TDAE oil to the S-SBR and BR.

(b) In the oil-extended BR compounds, a slight increase in T_g is observed by the DMA method with addition of every 10 phr of the TDAE oil. This is also an expected result based on the Fox's inverse rule of perfect mixtures considering the difference in the T_g of the S-SBR and the T_g of the TDAE oil. Therefore, an anti-plasticization effect of the TDAE is observed from the DMA method and supported by the theoretical prediction from Fox's inverse rule for perfect mixtures: see Fig. 9B. From the BDS and the PALS methods, the influence of the TDAE oil is considered individually for the amorphous-rich and the crystallite-rich BR phases. By adding TDAE oil, a slight decrease in the T_g of the amorphous-rich BR can be observed with both methods, BDS and PALS. However, the magnitude of this decrease is negligible. In addition, it is crucial to recognize that the value of T_g from the BDS method is obtained through an extrapolation of the data points using the VFT fitting protocol: see Fig. 3B. In the case of the amorphous-rich BR phase, there are few points available for the VFT fitting which makes it challenging to achieve a reliable extrapolation of the data points. It is more reliable to consider the shift of the data points corresponding to the segmental dynamics of the amorphous-rich BR phase along the x-axis (inverse of temperature). On considering this shift to see the influence of the TDAE on the segmental dynamics (T_g) of the amorphous-rich BR phase, a slight restrictive effect of the oil is noticed: see Fig. 9B. From the PALS method, it was noted for the amorphous-rich BR that the fractional free volume at the T_g remained unchanged: Fig. 7D–F. For the sake of comparison, the influence of the TDAE on the crystallite-rich BR is also judged by considering the shift of the data points corresponding to the segmental dynamics of this phase along the x-axis (inverse of temperature). A slight restrictive effect is seen for the segmental dynamics of the crystallite-rich BR with the addition of the TDAE oil. Thus, from the BDS method, a plasticization of the amorphous-rich and an anti-plasticization of the crystallite-rich BR is observed. From the PALS method, it was noted for the crystallite-rich BR that the fractional free volume at the T_g decreased slightly: Fig. 7D–F. It is likely that the incorporation of the TDAE oil slows down the increase in the fractional free volume of the oil-extended BR compounds between the T_g and the T_C by occupying the free volume sites. This results in a net decrease in the fractional free volume of the oil-extended BR compounds.

Table 7
T_g values for S-SBR/BR 70/30 wt ratio with 0/10/20 phr TDAE from DMA, BDS and PALS (with uncertainty of Tg-PALS of ±1.2 °C).

Compound	T_g^{DMA}/°C	T_g^{BDS}/°C	T_g^{PALS}/°C	F_v
70/30_0	−34	−52	−50	0.025
70/30_10	−36	−54	−50	0.028
70/30_20	−36	−53	−50	0.028

The influence of the TDAE oil on the BR compounds as observed from DMA, BDS and PALS has several contradictory inferences. However, the magnitude of all the observations (summarized in Fig. 9B and C and Table S6) is quite small. Therefore, it is concluded that there is no significant influence of the TDAE oil on the pure BR.

(c) In the oil-extended S-SBR/BR 70/30 blend, little or no effect of the addition of 10 and 20 phr of TDAE is observed on the T_g measured by all three methods (DMA, BDS and PALS): see Table 7. A slight shift in the T_g of the oil-extended 70/30 blend from the DMA method is an expected result based on Fox's inverse rule of perfect mixtures considering the difference in the T_g of the 70/30 from DMA (−34 °C) and the T_g of the TDAE oil (−49 °C). No significant shift in the T_g of the oil-extended 70/30 blends was observed from the BDS and the PALS methods: see Table 7. However, from the PALS measurements, an

Table 8
T_g values for the 50/50 blend with 0/10/20 phr TDAE oil from DMA and BDS measurements.

Compound	T_g^{DMA}/°C	T_g^{BDS}/°C
50/50_0	−54	−74
50/50_10	−53	−73
50/50_20	−52	−71

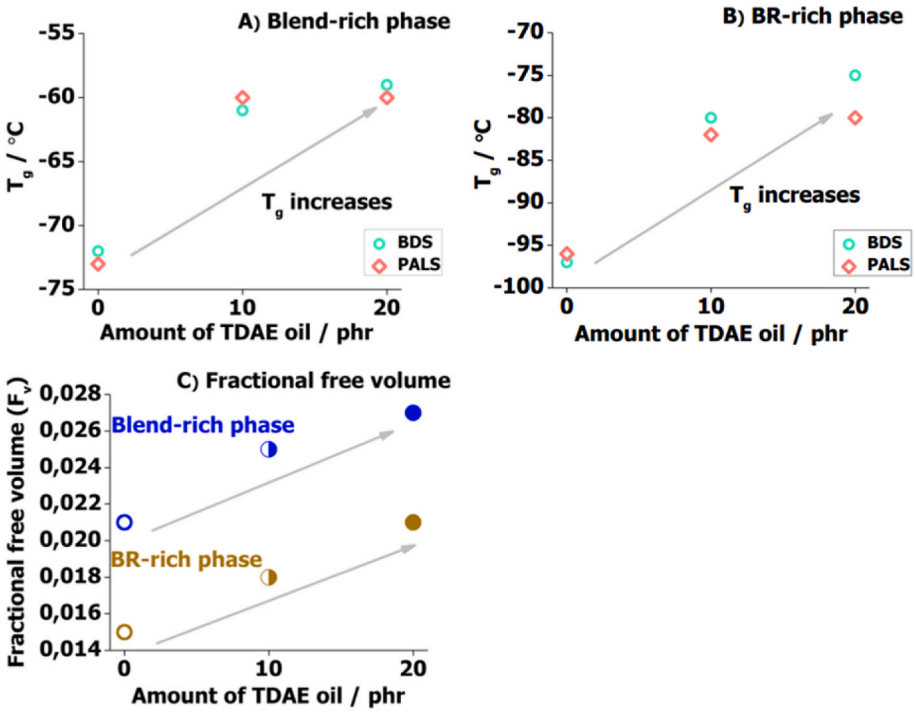

Fig. 10. Comparison of the shift in T_g from BDS (2 HN eqn. consideration) and PALS on the addition of the 0/10/20 phr pf TDAE oil to the A) Blend-rich phase, B) BR-rich phase, and C) a shift on the fractional free volume of the both phases of the S-SBR/BR.

accompanying increase in the fractional free volume at the T_g could also be seen. It can be considered that the T_g of the oil-extended 70/30 blend is the same for the non-oil-extended 70/30 blend due to the strong physical interactions between the blended (and possible interpenetrated) S-SBR and BR chains which cannot be modified by the addition of 10 and 20 phr TDAE oil. However, the accompanying fractional free volume at T_g increases with the addition of the oil in order to accommodate the oil molecules.

(d) In the case of the TDAE oil on the S-SBR/BR 50/50 blend (one HN eqn. consideration), the DMA and BDS results indicate that the T_g of this compound moves to higher temperatures with the addition of 20 phr of TDAE oil. The T_g values from the DMA and the BDS method are presented in Table 8. It is also possible to explain this effect based on Fox's rule of perfect mixtures which indicates that the T_g of the oil-extended compound should be an inverse weighted average of the component T_g's [6].

The T_g values from the BDS (two HN eqn. consideration) and the PALS method of TDAE oil on the S-SBR/BR 50/50 blend are coherent for the blend-rich and the BR-rich phases: see Fig. 10 and Table 7. The conclusion from these measurements is that by adding 10 and 20 phr TDAE oil to the 50/50 blend there is an increase in the T_g of both phases. The magnitude of this increase is higher in the BR-rich phase than in the blend-rich phase: Fig. 10A and B and Table 7. Surprisingly, a steady increase in the F_v at T_g of each phase is noticed on the addition of the 10 and 20 phr oil to the 50/50 blend. A possible explanation for these observations is that the inclusion of the bulky TDAE oil molecules in the blends increases the fractional free volume by pushing the chains apart but restricts the segmental mobility thereby increasing the T_g. Additionally, based on Fox's inverse rule of mixtures an increase in the T_g of both phases is expected as the T_g of both phases (−96 and −72 °C) in the non-oil-extended blend is lower than the Tg of the TDAE oil itself (−49 °C). Overall, it is noticed from the magnitude of the increase in the T_g and the corresponding F_v at T_g that there is a slight preference of the TDAE oil for the BR phase of the blend.

5. Conclusions

The HVLS S-SBR, high *cis*-BR and their blends in the 70/30 and 50/50 wt ratios have been studied for the influence of the addition of 0/10/20 phr of the TDAE on their T_g's by using DMA, BDS and PALS. An effect of the oil on the free volume of the compounds can be seen using the PALS method.

In S-SBR, the addition of TDAE leads to a decrease in the T_g of the compound and an increase in the F_v indicating an increase in mobility of the S-SBR chains as well as an extension of the free volume. This is an overall plasticization effect of the TDAE-extended S-SBR compounds. In BR, the addition of the TDAE oil leads to an increase in the T_g of the compound without a change in the corresponding F_v at T_g indicating a loss of the mobility of the BR chains while having no effect on the free volume. This means an anti-plasticization effect on the segmental dynamics.

In the 70/30 blend, the addition of the TDAE oil does not have any effect on the Tg of the compound but results in an increase in the Fv. This is possibly because the interactions between the S-SBR and BR component in the 70/30 blend are strong enough (high miscibility) to prevent the change in segmental dynamics. There is only an increase in the fractional free volume of the 70/30 blend with the addition of the TDAE oil.

For the 50/50 blend, it is possible to see the effect of the TDAE oil based on: i) the one HN equation consideration and ii) the two HN equation consideration of the blend. In the one HN equation consideration, a slight increase in the T_g and a corresponding increase in the fractional free volume is seen with the addition of the TDAE oil. In the two HN equation consideration, an increase in both the T_g and the corresponding F_v at T_g of each phase is noted. This means there is an anti-plasticization effect on the segmental dynamics and an increase of the free volume. The same trend can be seen from the one HN equation and the two HN equation consideration. From the Δ Tg values from the two HN equation consideration, there is a preference for the BR-rich phase by the oil.

Overall, the effect of the TDAE oil is seen to be governed by Fox's

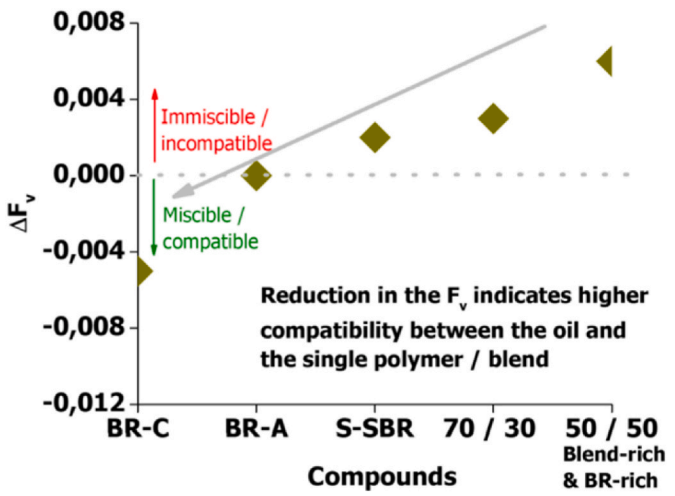

Fig. 11. Correlation between the change in fractional free volume (ΔF_v) and the different single polymer and blends studied in this chapter. The ΔF_v (F_v of oil-extended system – F_v of non-oil extended system) is calculated by subtracting the F_v of the non-oil-extended single polymer/blend from the Fv of the TDAE-oil-extended single polymer/blend, respectively.

inverse rule of mixtures regarding the direction of shift of the T_g. It leads to plasticization or anti-plasticization effect on the segmental dynamics of the compounds depending on the difference in T_g of the oil and the polymers. Also, there seems to be a correlation between the change in the fractional free volume and the compatibility of the oil and the single polymer/blend system: see Fig. 11. The change in the fractional free volume for the crystallite-rich phase of BR is negative, which means that the free volume of the oil-extended system is lower than the non-oil extended one. In terms of thermodynamics, a reduction in the free volume indicates a decrease in Gibb's free energy which is a general criterion for a blend to be miscible and vice-versa [43]. Therefore, it can be concluded from Fig. 11 that the compatibility of the TDAE with the various systems studied in this chapter is as follows: Crystallite-rich BR > Amorphous-rich BR > S-SBR > S-SBR/BR 70/30 > S-SBR/BR 50/50.

CRediT authorship contribution statement

Akansha Rathi: Writing – review & editing, Writing – original draft, Software, Formal analysis, Data curation, Conceptualization. **Pilar Bernal-Ortega:** Writing – original draft, Formal analysis, Data curation, Conceptualization. **Ahmed G. Attallah:** Writing – review & editing, Writing – original draft, Validation, Formal analysis, Data curation. **Reinhard Krause-Rehberg:** Writing – review & editing, Validation, Supervision, Funding acquisition. **Mohamed Elsayed:** Writing – review & editing, Validation, Formal analysis, Data curation, Conceptualization. **Jürgen Trimbach:** Writing – review & editing, Resources, Conceptualization. **Cristina Bergmann:** Writing – review & editing, Resources, Conceptualization. **Anke Blume:** Writing – review & editing, Validation, Supervision, Resources, Project administration, Investigation, Funding acquisition, Conceptualization.

Declaration of competing interest

The authors declare that they have no known competing financial interests or personal relationships that could have appeared to influence the work reported in this paper.

Data availability

Data will be made available on request.

Appendix A. Supplementary data

Supplementary data to this article can be found online at https://doi.org/10.1016/j.polymer.2024.127359.

References

[1] K.H. Nordsiek, Model studies for the developmemnt of an ideal tire tread, in: ACS Rubber Division Meeting, 1984. Indianapolis, U.S.A.
[2] K.H. Nordsiek, Entwicklung und Bedeutung spezieller Homopolymerisate des Butadiens, 25, Kautschuk Gummi Kunststoffe, 1972, pp. 87–92.
[3] Tire Technology Expo 2024, (n.d.). https://www.tiretechnology-expo.com/en/conference-program.php?day=all#programme (accessed March 23, 2024).
[4] A. Petchkaew, K. Sahakaro, J.W.M. Noordermeer, Petroleum-based Safe Process Oils in NR, SBR and Their Blends: Study on Unfilled Compounds. Part II. Properties, 66, KGK Kautschuk Gummi Kunststoffe, 2013.
[5] H.W. Engels, et al., Rubber, 9. Chemicals and Additives, Ullmann's Encyclopedia of Industrial Chemistry, Wiley-VCH Verlag GmbH & Co. KGaA, Weinheim, Germany, 2011.
[6] F.T. G., Influence of diluent and of copolymer composition on the glass temperature of a poly-mer system, Bull. Am. Phys. Soc. 1 (1956) 123. https://cir.nii.ac.jp/crid/1570572699490512512.bib?lang=en. (Accessed 3 August 2023).
[7] T.G. Fox, P.J. Flory, Second-order transition temperatures and related properties of polystyrene. I. Influence of molecular weight, J. Appl. Phys. 21 (1950) 581–591, https://doi.org/10.1063/1.1699711.
[8] D. Feldman, Polymer chemistry—the basic concepts, P. C. Hiemenz, Marcel Dekker, New York, 1984, 738 pp. No price given, J. Polym. Sci. Polym. Lett. Ed. 22 (1984) 673, https://doi.org/10.1002/pol.1984.130221208.
[9] P. Jia, H. Xia, K. Tang, Y. Zhou, Plasticizers derived from biomass Resources: a short review, Polymers 10 (2018), https://doi.org/10.3390/POLYM10121303.
[10] K. Sahakaro, A. Beraheng, Epoxidized natural oils as the alternative safe process oils in rubber compounds, Rubber Chem. Technol. 84 (2011) 200–214, https://doi.org/10.5254/1.3577518.
[11] W. Pechurai, W. Chiangta, P. Tharuen, Effect of vegetable oils as processing aids in SBR compounds, Macromol. Symp. 354 (2015) 191–196, https://doi.org/10.1002/MASY.201400079.
[12] S. Sökmen, K. Oßwald, K. Reincke, S. Ilisch, Influence of treated distillate aromatic Extract (TDAE) content and addition time on rubber-filler interactions in silica filled SBR/BR blends, Polymers 13 (2021) 698, https://doi.org/10.3390/POLYM13050698, 2021, Vol. 13, Page 698.
[13] A. Rathi, M. Hernández, W.K. Dierkes, J.W.M. Noordermeer, C. Bergmann, J. Trimbach, A. Blume, Effect of Aromatic Oil on Phase Dynamics of S-SBR/BR Blends for Passenger Car Tire Treads, 2016, pp. 1–33. https://research.utwente.nl/en/publications/effect-of-aromatic-oil-on-phase-dynamics-of-s-sbrbr-blends-for-pa. (Accessed 6 June 2024).
[14] A. Rathi, M. Hern, S.J. Garcia, W.K. Dierkes, J.W.M. Noordermeer, C. Bergmann, J. Urgen Trimbach, A. Blume, Identifying the effect of aromatic oil on the individual component dynamics of S-SBR/BR blends by broadband dielectric spectroscopy, J. Polym. Sci., Part B: Polym. Phys. 56 (2018) 842–854, https://doi.org/10.1002/polb.24599.
[15] D. Kilburn, G. Dlubek, J. Pionteck, M.A. Alam, Free volume in poly(n-alkyl methacrylate)s from positron lifetime and PVT experiments and its relation to the structural relaxation, Polymer (Guildf). 47 (2006) 7774–7785, https://doi.org/10.1016/J.POLYMER.2006.08.055.
[16] G. Dlubek, A. Sen Gupta, J. Pionteck, R. Krause-Rehberg, H. Kaspar, K. Helmut Lochhaas, Temperature dependence of the free volume in fluoroelastomers from positron lifetime and PVT experiments, Macromolecules 37 (2004) 6606–6618, https://doi.org/10.1021/MA049067N/SUPPL_FILE/MA049067NSI20040621_113149.PDF.
[17] D. Kilburn, D. Bamford, T. Lüpke, G. Dlubek, T.J. Menke, M.A. Alam, Free volume and glass transition in ethylene/1-octene copolymers: positron lifetime studies and dynamic mechanical analysis, Polymer (Guildf). 43 (2002) 6973–6983, https://doi.org/10.1016/S0032-3861(02)00663-8.
[18] G. Dlubek, J. Pionteck, Y. Yu, S. Thränert, M. Elsayed, E. Badawi, R. Krause-Rehberg, The free volume and its recovery in pressure-densified and CO 2-swollen heterocyclic-ring-containing fluoropolymersa, Macromol. Chem. Phys. 209 (2008), https://doi.org/10.1002/macp.200800189.
[19] M. Elsayed, R. Krause-Rehberg, B. Korff, S. Richter, H.S. Leipner, Identification of as-vacancy complexes in Zn-diffused GaAs, J. Appl. Phys. 113 (2013), https://doi.org/10.1063/1.4793791.
[20] M. Elsayed, R. Krause-Rehberg, O. Moutanabbir, W. Anwand, S. Richter, C. Hagendorf, Cu diffusion-induced vacancy-like defects in freestanding GaN, New J. Phys. 13 (2011), https://doi.org/10.1088/1367-2630/13/1/013029.
[21] F. Lotter, U. Muehle, M. Elsayed, A.M. Ibrahim, T. Schubert, R. Krause-Rehberg, B. Kieback, T.E.M. Staab, Precipitation behavior in high-purity aluminium alloys with trace elements – the role of quenched-in vacancies, Phys. Status Solidi Appl. Mater. Sci. 215 (2018) 1–11, https://doi.org/10.1002/pssa.201800375.
[22] M. Elsayed, T.E.M. Staab, J. Čížek, R. Krause-Rehberg, Monovacancy-hydrogen interaction in pure aluminum: experimental and ab-initio theoretical positron annihilation study, Acta Mater. 248 (2023) 118770, https://doi.org/10.1016/j.actamat.2023.118770.
[23] J. Kansy, Microcomputer program for analysis of positron annihilation lifetime spectra, Nucl. Instruments Methods Phys. Res. Sect. A Accel. Spectrometers, Detect.

Assoc. Equip. 374 (1996) 235–244, https://doi.org/10.1016/0168-9002(96)00075-7.
[24] A. Rathi, W.K. Dierkes, A. Blume, M. Hernández, C. Bergmann, J. Trimbach, Structure–property relationships of 'safe' aromatic oil based passenger car tire tread rubber compounds, KGK - Kautsch. Gummi Kunstst. 69 (2016) 22–27. https://research.utwente.nl/en/publications/structureproperty-relationships-of-safe-aromatic-oil-based-passen. (Accessed 15 June 2024).
[25] A. Rathi, Investigating safe mineral-based and bio-based process oils for tire tread application. https://doi.org/10.3990/1.9789036548854, 2019.
[26] L. Mandelkern, Crystallization of Polymers: Volume 2: Kinetics and Mechanisms, second ed., Cambridge University Press, Cambridge, 2004 https://doi.org/10.1017/CBO9780511535413.
[27] M. Wunde, M. Klüppel, Effect of filler and blending with SBR and NR on thermally induced crystallization of high-cis BR as evaluated by dynamic mechanical analysis, Express Polym. Lett. 14 (2020) 261–271, https://doi.org/10.3144/EXPRESSPOLYMLETT.2020.22.
[28] D. Hao, D. Li, Determination of dynamic mechanical properties of carbon black filled rubbers at wide frequency range using Havriliak–Negami model, Eur. J. Mech. Solid. 53 (2015) 303–310, https://doi.org/10.1016/J.EUROMECHSOL.2015.06.002.
[29] N. Metatla, A. Soldera, The Vogel-Fulcher-Tamman equation investigated by atomistic simulation with regard to the Adam-Gibbs model, Macromolecules 40 (2007) 9680–9685, https://doi.org/10.1021/MA071788.
[30] R.H. Schuster, H.M. Issel, V. Peterseim, Selective interactions in elastomers, a base for compatibility and polymer-filler interactions, Rubber Chem. Technol. 69 (1996), https://doi.org/10.5254/1.3538400.
[31] D. Turnbull, M.H. Cohen, On the free-volume model of the liquid-glass transition, J. Chem. Phys. 52 (1970) 3038–3041, https://doi.org/10.1063/1.1673434.
[32] M.H. Cohen, D. Turnbull, Molecular transport in liquids and glasses, J. Chem. Phys. 31 (1959) 1164–1169, https://doi.org/10.1063/1.1730566.
[33] D. Turnbull, M.H. Cohen, Free-volume model of the amorphous phase: glass transition, J. Chem. Phys. 34 (1961) 120–125, https://doi.org/10.1063/1.1731549.
[34] J. P, James P. Runt, J.J. Fitzgerald, Dielectric Spectroscopy of Polymeric Materials : Fundamentals and Applications, 1997, p. 461.
[35] C.A. Angell, Relaxation in liquids, polymers and plastic crystals — strong/fragile patterns and problems, J. Non-Cryst. Solids 131–133 (1991) 13–31, https://doi.org/10.1016/0022-3093(91)90266-9.
[36] A. Schönhals, F. Kremer, Analysis of dielectric spectra, broadband dielectr, Spectroscopy (Amsterdam, Neth.) (2003) 59–98, https://doi.org/10.1007/978-3-642-56120-7_3.
[37] G.A. Schwartz, L. Ortega, M. Meyer, N.A. Isitman, C. Sill, S. Westermann, S. Cerveny, Extended adam-gibbs approach to describe the segmental dynamics of cross-linked miscible rubber blends, Macromolecules 51 (2018) 1741–1747, https://doi.org/10.1021/ACS.MACROMOL.7B02432.
[38] G.-C. Chung, Segmental dynamics of individual species in a miscible polymer blend. https://doi.org/10.7907/DP5V-GT76, 1995.
[39] R.S. Porter, Polymer chemistry—the basic concepts: by Paul C. Hiemenz, Dekker, New York, 1984. 752 pp. $34.50, J. Colloid Interface Sci. 109 (1986) 594, https://doi.org/10.1016/0021-9797(86)90343-7.
[40] W. Salgueiro, A. Somoza, L. Silva, G. Consolati, F. Quasso, M.A. Mansilla, A. J. Marzocca, Temperature dependence on free volume in cured natural rubber and styrene-butadiene rubber blends, Phys. Rev. E. 83 (2011), https://doi.org/10.1103/physreve.83.051805.
[41] D. Račko, R. Chelli, G. Cardini, J. Bartoš, S. Califano, Insights into positron annihilation lifetime spectroscopy by molecular dynamics simulations, Eur. Phys. J. D - At. Mol. Opt. Plasma Phys 32 (2005) 289–297, https://doi.org/10.1140/epjd/e2005-00015-y.
[42] J. Bartos, O. Sausa, J. Kristiak, T. Blochowicz, E. Rössler, Free-volume microstructure of glycerol and its supercooled liquid-state dynamics, J. Phys. Condens. Matter 13 (2001) 11473–11484, https://doi.org/10.1088/0953-8984/13/50/307.
[43] J. Liu, Y.C. Jean, H. Yang, Free-volume hole properties of polymer blends probed by positron annihilation spectroscopy: miscibility, Macromolecules 28 (1995) 5774–5779, https://doi.org/10.1021/ma00121a012.